A Three-Port Interface Converter by Using an Indirect Matrix Converter with the Neutral Point of the Motor

Goh Teck Chiang
Student Member, IEEE
Nagaoka University of Technology
1603-1 Kamitomioka,
Nagaoka Niigata, 940-2188, Japan
tcgoh@stn.nagaokaut.ac.jp

Jun-ichi Itoh
Senior Member, IEEE
Nagaoka University of Technology
1603-1 Kamitomioka,
Nagaoka Niigata, 940-2188, Japan
itoh@vos.nagaokaut.ac.jp

***Abstract* – This paper proposes a new three-phase power system that is applicable in various motor drive systems including HEV. The main circuit is based on an Indirect Matrix Converter (IMC) and the neutral point connection of a motor is utilized by connecting to an additional DC/DC converter. The DC link part of the IMC connects a boost-up type DC/DC converter and batteries to perform as a secondary power source to drive the motor. In addition, the proposed control method can utilize the leakage inductance of a motor as a boost-up reactor which will replace a common reactor in a boost-up chopper. The proposed converter has been simulated and validated experimentally using a 750W-prototype that driven by an induction motor with V/f control. The total harmonic distortion (THD) of the input current is 4%, the THD of the output current is 3.7% and the efficiency is 96%.**

***Index Terms*— Indirect Matrix Converter, DC/DC Boost Converter, Leakage inductance of a motor, Neutral point connection of a motor, Zero vectors, Positive-phase sequence, Negative-phase sequence**

I. INTRODUCTION

Environmental responsibility has been a great concern for communities. The developments of the renewable power energies, such as wind turbines and Hybrid Electric Vehicles (HEVs), are growing rapidly. One of the most common applied converters in hybrid systems is AC/DC/AC converter because it has the ability for connection of two different power sources. The generator mainly supplies a constant power to the load and the battery is used as an alternate power to drive an electric motor and also to absorb the power fluctuation at the high peak energy demands.

Fig.1 shows a conventional AC/DC/AC power converter typically consists of a PWM rectifier, a DC link capacitor and a PWM inverter, also known as the back to back (BTB) system [1]. The PWM rectifier is often used to reduce the harmonic currents in a generator and to control the DC link voltage [2-5]. In order to obtain high performance under an adjustable speed drive system, a constant DC link voltage is required in a BTB system because the voltage fluctuation of the DC link part will cause an output voltage error. A typical method of reducing the voltage fluctuation is to place a large electrolytic capacitor into the DC link part as a filtering device between the rectifier and the inverter. However, the large electrolytic capacitor has a relatively limited operating lifetime and high maintenance cost.

One of the approaches uses to reduce the capacity of the electrolytic capacitor is by applying a high speed DC voltage controller into the rectifier control [6]. However, the control response is limited by the delay of the voltage detection and a digital controller, the electrolytic capacitor is still required. In addition, the capacitor is reduced when the DC link capacitor is dominated by the capacitor current. As a result, a large amount of space is needed for installing the capacitor in a real product. Especially, the electrolytic capacitor is not suitable for the high temperature installation such as in HEV. These disadvantages are affecting the reliability of the converter.

For the secondary input power source, a boost converter consists of batteries and a boost-up reactor is connected to the DC link part of BTB. The boost converter increases the battery voltage, and then injects the battery power into the DC link part. Many studies in wind turbines [7]-[9] have shown that in a DC/DC boost converter, the boost-up reactor depends on the switching frequency and the current response and these factors are limited by the efficiency and controller. As a result, a large boost-up reactor is required.

This paper demonstrates and describes a new circuit topology which composed of an indirect matrix converter and a DC/DC boost converter that connects to the neutral point of a motor. Indirect matrix converter is high efficiency and easy to configure in compared with the conventional method [10]-[13]. It does not require a DC link electrolytic capacitor to maintain a stable DC link voltage.

Furthermore, this paper proposes an appropriate control over the inverter that is possible to connect the DC chopper to the neutral point of a motor and to operate as a DC/DC converter [14]. The proposed circuit utilizes the neutral point of a motor in the boost converter because the leakage inductance of the motor can be used as a reactor. By removing the electrolytic capacitor and the boost-up reactor, the remaining part of the proposed circuit is only constructed by silicon components which are the IGBTs.

As a result, the proposed circuit is low cost and high reliability. The simulation results and the experimental results clearly demonstrate that the proposed circuit is capable of providing sinusoidal waveforms for the input and the output and achieves high efficiency and high power factor.

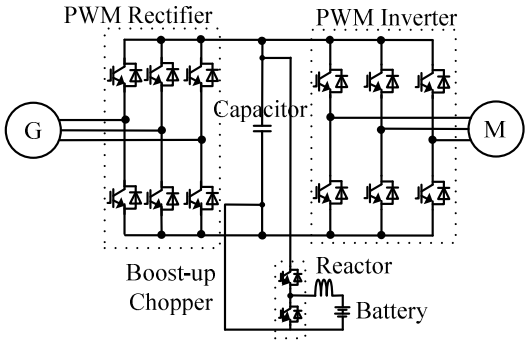

Fig. 1. Back to Back converter.

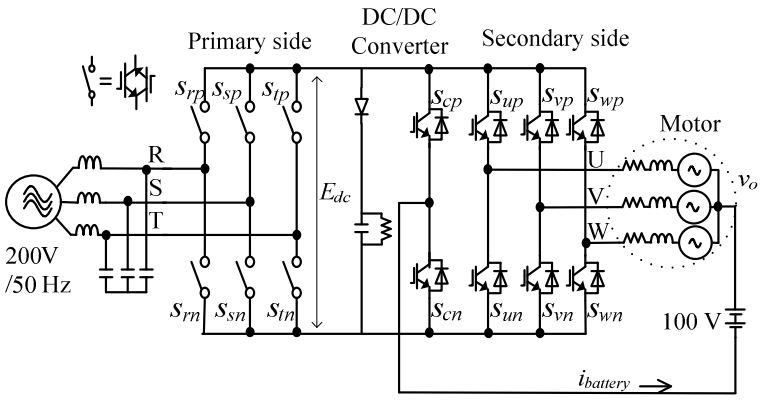

Fig. 2. Proposed circuit topology.

II. PROPOSED CIRCUIT TOPOLOGY

Fig.2 shows the proposed circuit configuration. The indirect matrix converter can be simply divided into primary stage and secondary stage. The primary stage for the AC power source consists of twelve units of reverse blocking IGBT [15] also known as a current source rectifier. The secondary stage for the motor consists of six units of IGBT, which is similar to a standard voltage source inverter. The indirect matrix converter has one advantage over a matrix converter is to having a DC link part. In the proposed method, the DC link part is utilized by adding a boost converter into the indirect matrix converter. The boost converter connects to the battery, and then the other terminal of the battery is connected to the neutral point of a motor. Moreover, a snubber circuit is included in the DC link part to absorb energy from the reactive elements in the circuit such as voltage overshoot [15]. It should be noted that the capacity of the snubber capacitor is smaller than the DC link capacitor in a BTB system because the ripple current of the DC link part does not flow in the snubber capacitor.

The boost converter is not a stand-alone circuit in this proposed circuit. The operation is strongly depended on the secondary side of the indirect matrix converter. Zero vectors output in the secondary side are the key factor to link the boost converter into the indirect matrix converter. The zero vector controls the amplitude of the output voltage. Besides, there are two functions of the zero vectors output into the secondary side. The first is to implement zero current switching on the primary side, so the switching losses at primary side do not occur. The second involves in the operation of the boost converter, which will be descried in the later chapter.

III. CONTROL BLOCK DIAGRAM

Fig. 3 shows the control block diagram of the proposed circuit. The primary side, the DC chopper and the secondary side are controlled individually by their own commands. A carrier comparison method is used as the PWM generator according to the control strategy [16]. The relations between the output voltage and the input voltage are obtained by (1). The secondary side operates as a four-phase voltage source inverter by adding the DC chopper as the fourth leg,

$$\begin{bmatrix} v_u \\ v_v \\ v_w \\ v_c \end{bmatrix} = \begin{bmatrix} s_{up} & s_{un} \\ s_{vp} & s_{vn} \\ s_{wp} & s_{wn} \\ s_{cp} & s_{cn} \end{bmatrix} \begin{bmatrix} s_{rp} & s_{sp} & s_{tp} \\ s_{rn} & s_{sn} & s_{tn} \end{bmatrix} \begin{bmatrix} v_r \\ v_s \\ v_t \end{bmatrix}. \tag{1}$$

where s_{xy} stands for the switching function of the switches. When s_{xy} is turned on, $s_{xy} = 1$ and when s_{xy} is turned off, $s_{xy} = 0$.

The primary side controller is designed with a current type PWM rectifier command. It is a pulse pattern conversion to convert the PWM pulses of the voltage source type rectifier into the PWM pulse of the current source type rectifier. A stable DC link voltage can be achieved by using this method. Further, the single leg modulation is used to reduce the switching losses to $\pi/3$ per period [15].

A conventional controller method for voltage source type inverter is applied to the DC chopper and the inverter with a lean controlled carrier modulation. This carrier modulation forms a new carrier where the peak position of the triangle carrier is controlled by the duty ratio of the rectifier side pulse. Then, this new carrier is used in the secondary side and the DC chopper as a normal PWM comparison method. It also called as inverter carrier.

Additionally, a PI controller is designed in the DC chopper to control the battery current. Note that since the DC chopper is controlled as the fourth leg of the inverter, the DC chopper command is compared by the same carrier with the inverter voltage commands. Fig. 3 shows the control block diagram which is explaining above.

Fig. 4 shows an example of the relations between the normal carrier applied into the primary side and the new inverter carrier applied into the secondary side. There are two ways to generate an inverter carrier; Fig. 4(a) represents the symmetrical type which contains approximately double switching frequency of the rectifier switching frequency and Fig. 4(b) shows the asymmetrical way which contains the

same switching frequency of the rectifier switching frequency [17].

In Fig. 4(a), the bottom peak position of the triangular carrier is controlled by the duty ratio of the rectifier pulse as shown at the upper graph. The chopper commands along with the inverter output voltage commands are compared with this new inverter carrier to obtain the desired switching patterns. The zero vector periods are shown at the lower graph in Fig. 4(a). The switching pulses of the secondary side attained the zero vectors for every carrier cycle. The primary side arms will switch at every zero vector periods.

In addition, the upper arm of the chopper will switch ON at every zero vector periods. During zero vector periods, the boost converter is operated at On-state, the battery current will be charged thru by the leakage inductance of a motor. During the non-zero vector periods, the accumulated battery energy will be released into the indirect matrix converter, also known as the Off-state operation.

When the switching frequency of the rectifier is 10kHz, the applied control method generates a new carrier which contains approximately 20 kHz switching frequency at every carrier. It is approximately double of the primary side switching frequency. In Fig. 4(b), an inverter carrier can be formed that is based on the duty of the rectifier command but contains only 10 kHz per carrier cycle using a symmetrical carrier. This inverter carrier can improve the efficiency by reducing the switching losses in the inverter side and the chopper side.

By comparing between the symmetrical inverter carrier and the asymmetrical inverter carrier in Fig. 4, note that the zero current switching in the rectifier does not affect by the inverter carrier because both carrier are formed follow the rectifier duty. Since every carrier time is longer in the asymmetrical inverter carrier, the sequence of the zero vector periods becomes slower. That is, the boost converter will achieve a better efficiency, however the current ripple in the battery will be increased.

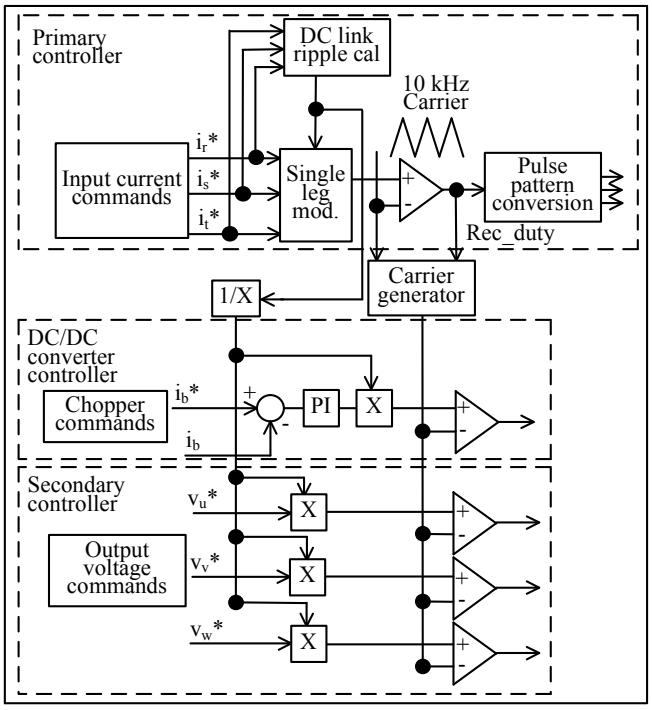

Fig. 3. Control block diagram.

The other disadvantage of the asymmetrical inverter carrier is the detection of the load current. Normally, the average value of the load current appears at the peak of the symmetrical inverter carrier. It can be easily detected by using symmetrical inverter carrier. However, in asymmetrical carrier, the average current point does not agree with the peak of the asymmetrical carrier. In order to detect the average current, a low-pass-filter is required. Consequently, performances of the control will be decreased.

IV. UTILIZATION OF THE NEUTRAL POING OF A MOTOR

The importance of the zero vectors explains the behavior of the boost converter along with the neutral point of the motor. The boost converter will operate at every zero vectors of the secondary side of the converter. A three-phase inverter has eight output voltage space vectors including two zero vectors. The zero vectors are two particular vectors that generate zero line voltage to the motor. The neutral point voltage v_0 of the motor based on the neutral point of the DC link part is obtained as (2)

$$\begin{cases} v_o = \dfrac{E_{dc}}{2} & \text{When all upper arms are ON} \\ v_o = \dfrac{-\mathrm{E_{dc}}}{2} & \text{When all lower arms are ON} \end{cases} \tag{2}$$

where E_{dc} is the DC link voltage and v_o is the voltage of the neutral point of the motor based on the neutral point of the DC link part.

The proposed circuit has two difference sequences during the zero vectors, a positive-phase sequence and a zero-phase sequence. Fig. 5 shows the positive-phase sequence equivalent circuit and Fig. 6 shows the zero-phase sequence equivalent circuit. In the positive-phase sequence, the secondary side works normally as a three-phase inverter with a motor. It will control the motor speed and torque.

On the other hand, in the zero-phase sequence, no voltage goes to the motor because the line voltage is zero and the motor can be considered as a leakage inductance. Additionally, the secondary side of the converter can be considered as a single leg topology. The battery current first goes into the secondary side and flows out through the neutral line and charge or discharge the battery. The battery current can be controlled by the PI controller. A new expression of the secondary side current is formed as follows

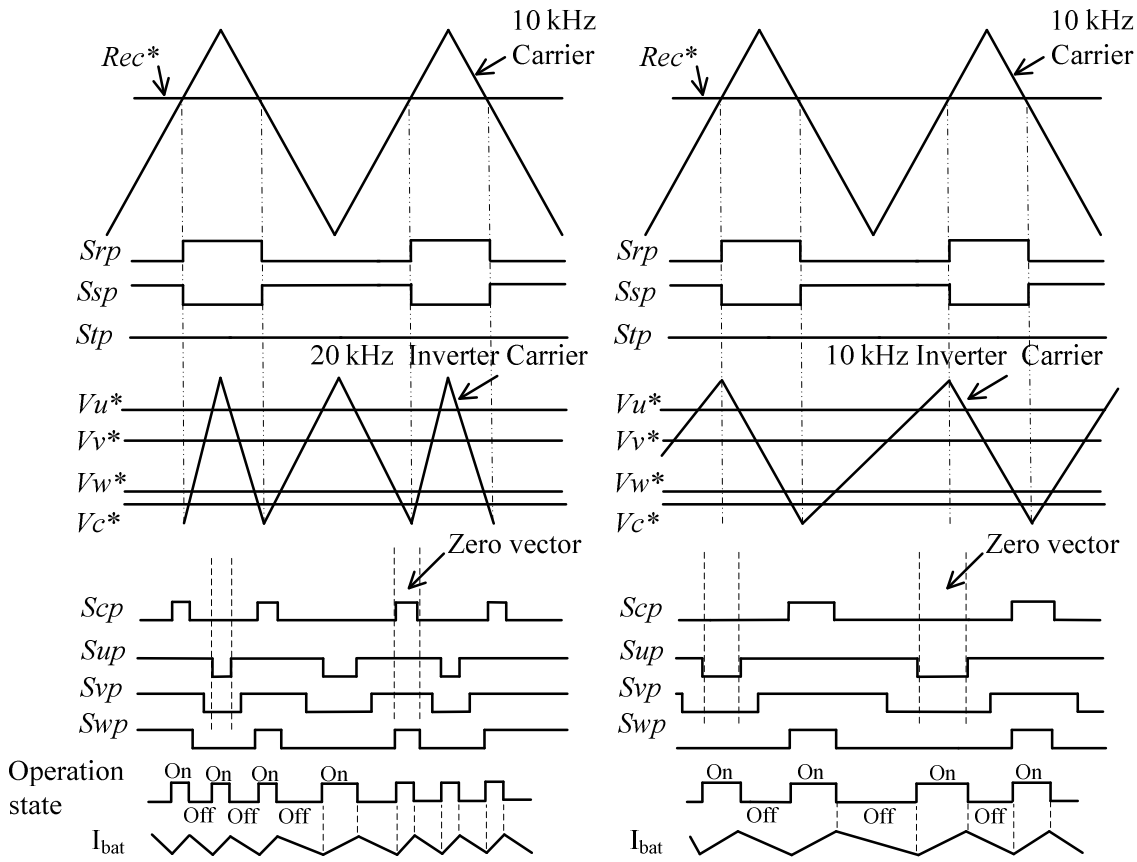

Fig. 4(a). Symmetrical inverter carrier. Fig. 4(b). Asymmetrical inverter carrier.

Fig. 4. Relations between the zero vectors and boost converter operation.

$$\begin{cases} i_u = i_a + \dfrac{i_{bat}}{3} \\ i_v = i_b + \dfrac{i_{bat}}{3} \\ i_w = i_c + \dfrac{i_{bat}}{3} \end{cases} . \quad (3)$$

where i_a, i_b, i_c are the inverter current and i_{bat} is the battery current;

Since high DC link voltage is compulsory in order to control the zero vectors, the relations between the DC link voltage E_{dc}, the inverter line voltage (v_{inv}) and the battery voltage (V_{bat}) will be discussed. The inverter output voltage, v_u, v_v, v_w referred to the neutral point voltage of the dc link is expressed as

$$\begin{cases} v_u = a\dfrac{E_{dc}}{2}\sin\omega t + v_o \\ v_v = a\dfrac{E_{dc}}{2}\sin(\omega t - \dfrac{2\pi}{3}) + v_o \\ v_w = a\dfrac{E_{dc}}{2}\sin(\omega t - \dfrac{4\pi}{3}) + v_o \end{cases} . \quad (4)$$

where

a is the modulation index of the motor phase voltage, $0 < a < 1$

v_o is neutral point voltage of the motor (during zero phase sequence) and ω is inverter output angler frequency

Then, the inverter line voltage is given by

$$v_{uv} = a\frac{\sqrt{3}}{2}V_{dc}\sin\omega t + \frac{\pi}{6}. \quad (5)$$

For a three-phase inverter, the DC link voltage E_{dc} is required as (6) when a sinusoidal modulation is used.

$$E_{dc} \geq 2\frac{\sqrt{2}}{\sqrt{3}}V_{inv} . \quad (6)$$

The maximum line voltage between the inverter leg and chopper leg can be obtained as

$$v_{ux} = \frac{\sqrt{2}}{\sqrt{3}}V_{inv} + V_{bat}. \quad (7)$$

Since v_{ux} must be smaller than E_{dc} , the inverter voltage and battery voltage are constrained by (8)

$$E_{dc} > \frac{\sqrt{2}}{\sqrt{3}}V_{inv} + V_{bat}. \quad (8)$$

As a result, the DC link voltage of the proposed circuit must satisfy both requirements as shown below

$$E_{dc} \geq \begin{cases} 2\frac{\sqrt{2}}{\sqrt{3}}V_{inv} & When \frac{\sqrt{2}V_{inv}}{\sqrt{3}} \geq V_{bat} \\ \frac{\sqrt{2}}{\sqrt{3}}V_{inv} + V_{bat} & When \frac{\sqrt{2}V_{inv}}{\sqrt{3}} < V_{bat} \end{cases} \quad (9)$$

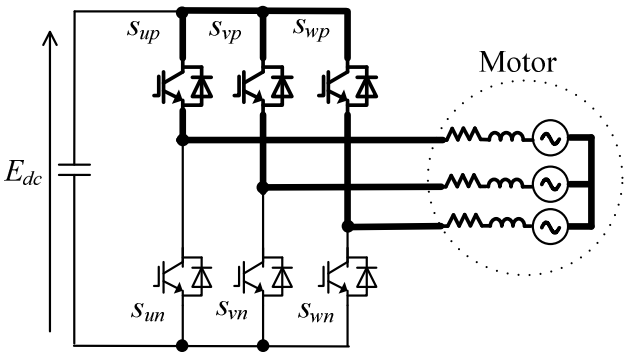

Fig. 5. Positive phase sequence equivalent circuit.

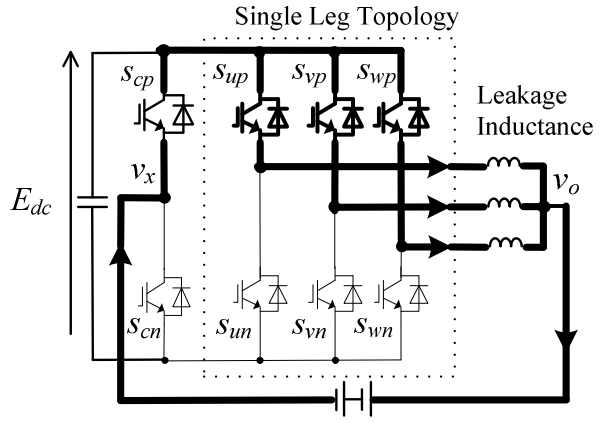

Fig. 6. Zero phase sequence equivalent circuit.

TABLE I
SIMULATION PARAMETERS

Input voltage	200 V
Input frequency	50 Hz
Carrier frequency	10 kHz
Inverter frequency	20 kHz
DC source	100 V
Output voltage	173 V
Output frequency	35 Hz
Leakage inductance	5 mH

V. SIMULATION RESULTS

Table I shows the simulation parameters for both results. The proposed circuit was simulated under two conditions; the battery discharging and charging. An ACR controller controls the battery current into a desired value of positive or negative. An ideal battery current i_b is purposely adjusted at specific time of 20 ms to confirm the proposed circuit performance. The motor model, which consists of three sets of voltage sources as back electro motive forces and leakage inductances, is used in the simulation. The symmetrical inverter carrier is used in simulation.

Fig. 7 shows the battery discharging mode where the battery current is controlled from 0.5 A to 2 A. These two waveforms show the input power supply voltages v_r, v_s, v_t , the input currents i_r, i_s, i_t, the output line voltages ($v_{uv(LPF)}$, $v_{vw(LPF)}$), $v_{wu(LPF)}$) through a low pass filter, which has the cut off frequency of 1 kHz, to observe the low frequency components, the output currents i_u, i_v, i_w and the battery current i_b. The results show that both the input current and output current are good sinusoidal waveforms. It should be noted that at time 20 ms, the input current magnitude decreases due to the increment of i_b, which means that the increasing of the battery power leads to a decreasing in generator power.

On the other hand, in Fig.8 the ACR controls the battery current to from 0.5 A to -2 A. The battery is being charged from a generator in this condition. The results also proved that when in charging mode, both the input current and output current obtain good sinusoidal waveforms. At 20 ms, as the i_b decreases, the input current forces to increase because a larger energy is required to charge the battery. These two waveforms proved a good power management picture between the generator and the battery.

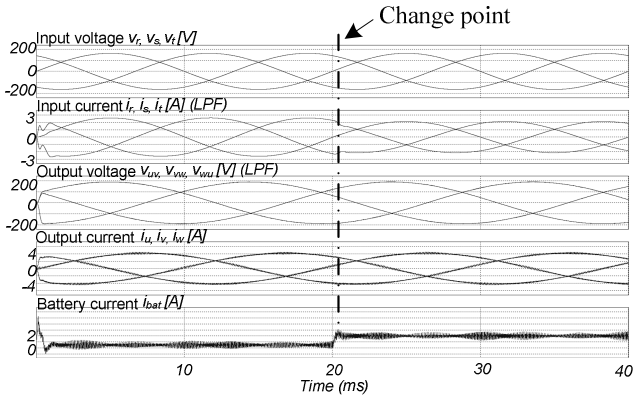

Fig. 7. Simulation results (Battery=Discharge mode).

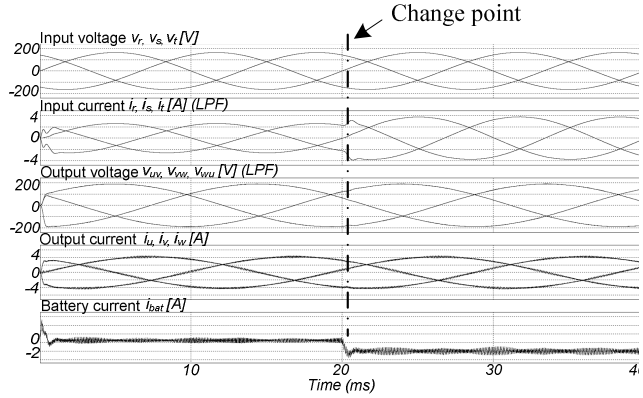

Fig. 8. Simulation results (Battery=Charge mode).

VI. EXPERIMENTAL RESULTS

A 750-W prototype was built and tested in two operation modes same to simulation section. Mode I is the battery discharges under motoring operation and Mode II is the battery charges under motoring operation. Both conditions were verified using the parameters shown in table II. The controller was using asymmetrical format to generate the 10-kHz inverter carrier. Indirect matrix converter can achieve a better THD values by applying this method. Table III shows the motor specification data. Note that it is an ordinary motor; no particular setting is required for the neutral point connection.

A. Fundamental Operations

Fig. 9 and Fig. 10 show the Mode I operation and the Mode II operation, respectively. In Fig. 9, the DC power supply is set to 100 V and the battery current is controlled to 2 A. Likewise in Fig. 10, the battery current is controlled to -2 A. Good sinusoidal waveforms have been achieved in the input and the output current of both operation modes. Fig. 11 shows the input power factor of discharge mode and charge mode. Both modes achieved the input power factor more than 98%, which can be considered as a unity power factor. The input power factor decreases during the discharge mode is because the input current becomes smaller in comparison with the charge mode.

Fig. 12 shows the input current total harmonics distortion (THD) and the output current THD for both modes. The lowest output current THD obtains during the charge mode is 3.6% and during discharge mode is 4.0%. As for the lowest output current THD obtains during the charge mode is 3.0% and during discharge mode is 3.7%.

B. Efficiency and Loss Analysis

This section will discuss the loss analysis of the proposed circuit which is calculated by using a circuit simulator (PSIM, *Powersim Technologies Inc.*) and DLL files (Dynamic Link Library) [18]. The analysis was conducted in two categories by applying the symmetrical and asymmetrical inverter carrier respectively. Figs. 13, 14, 15 and 16 show the loss analysis results simulated under the same parameter as shown in Table I. The output power is 750 W and the input power ratio is 9:1 in Figs. 13 and 14.

Fig. 13 shows the detail of the switching losses when applying the symmetrical inverter carrier. The zero current switching is implemented in the primary side, and therefore only conduction loss occurs into it. The total loss for the discharge mode is approximately 27 W and the total loss for the charge mode is approximately 29 W. The analysis proves that the converter can achieve an efficiency of 96.4%.

Two reasons are found about the higher losses in secondary side. The first reason is that the switching frequency in the secondary side is 20 kHz by using the symmetric method as discussed in chapter III. The second reason is because the inverter current contains of the battery current during zero phase sequence. Higher switching frequency and larger battery current resulted the losses are increasing.

Fig. 14 shows the asymmetric inverter carrier loss analysis results. It was simulated under the same condition with Fig. 13. The loss in secondary side decreases about 20% and the loss in chopper decreases about 25%. The total loss for the

TABLE II
EXPERIMENTAL PARAMETERS

Input voltage	200 V
Input frequency	50 Hz
Carrier frequency	10 kHz
Output frequency	35 Hz
Inductor	1.7 mH
Capacitor	2.5 μF
DC source	100 V
LC Filter Cut-off frequency	2.4 kHz

TABLE III
MOTOR PARAMETERS (FUJI: MLH6085M)

Motor Power	750 W
Poles	4/ 50 Hz
RPM	1420
Rated current	3.6 A
Rated voltage	200 V
Leakage inductance	4.42 mH

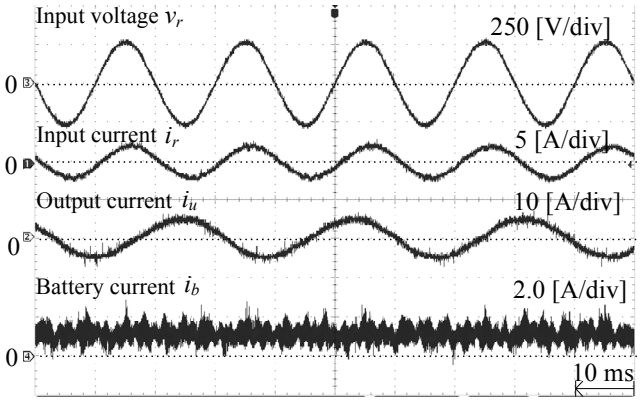

Fig. 9. Experimental result (Mode I= Battery discharge).

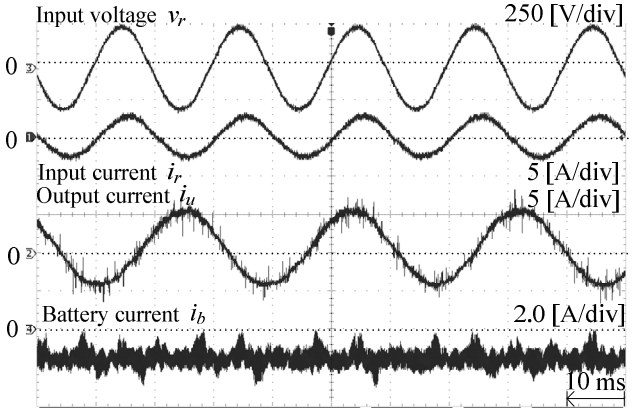

Fig. 10. Experimental result (Mode II = Battery charge).

discharge mode is 23 W and the total loss for charge mode is 25W. An efficiency of 96.9% can be achieved, which is approximately 0.5% improvement.

Fig. 15 and Fig. 16 show calculations of the loss analysis by powering with various input power ratio, as given from 10:0 to 1:9, where it represents the ratio of generator power to battery power. At the ratio 9:1, it means that the total input power is 90% supplied from the generator power and the remaining 10% from the battery power. In this case, the input voltage gradually reduces as the battery voltage increases.

In Fig. 15, the asymmetric method, it is obvious from the graph that the loss in the DC chopper increases sharply as the battery current increases. However, the loss in primary does not reach zero, it drops to a constant 4 W from 7 W.

On the other hand, as the generator power is lesser than 225 W, the loss in the secondary side starts to decrease. This is because in the indirect matrix converter, the output voltage ratio is directly depending on the input voltage. As the input voltage ratio decreases, the magnitude of the output voltage decreases as well. However in the proposed circuit, the boost converter maintains the DC link voltage even the generator power drops. Therefore, the output side can remain at its power.

Fig. 16 illustrates a chart that is the same analysis with the second condition but it applies the symmetric format. As expected, the loss in the primary side remains unchanged. However, the loss in secondary side reduces about 18% compared to Fig. 15. When the battery is at the full power, the loss reduces about 25%.

VII. CONCLUSION

This paper proposed a new control method by utilizing the neutral point of a motor and connected to an indirect matrix converter for motor drive applications. The control over the inverter zero vector periods allows an additional chopper leg to perform as a boost converter with the connection to the neutral point of a motor. The simulation and the experimental results demonstrated good sinusoidal waveforms and confirmed the validity of the proposed method. Furthermore, the loss analysis in the proposed circuit estimates efficiency of 96%.

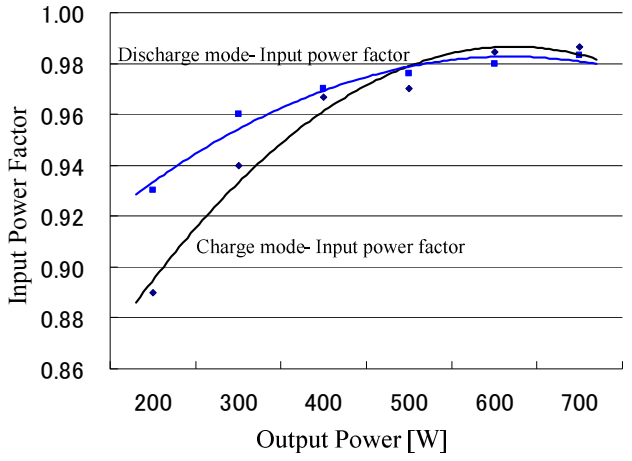

Fig. 11. Input power factor.

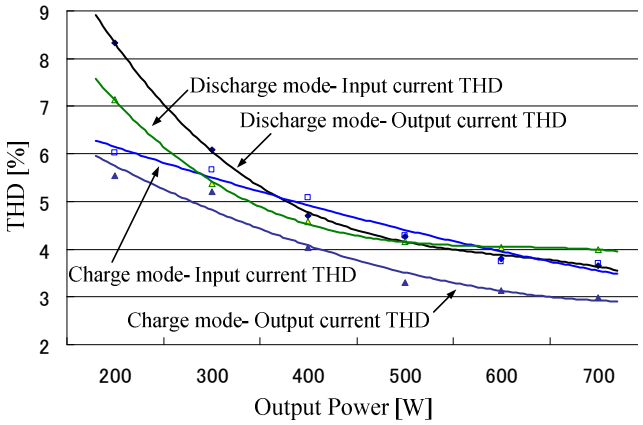

Fig. 12. Input & output current THD values.

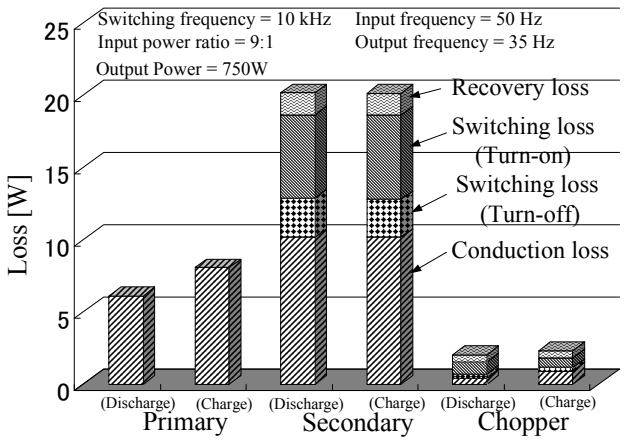

Fig. 13. Loss analysis – Switching device losses (Symmetric method).

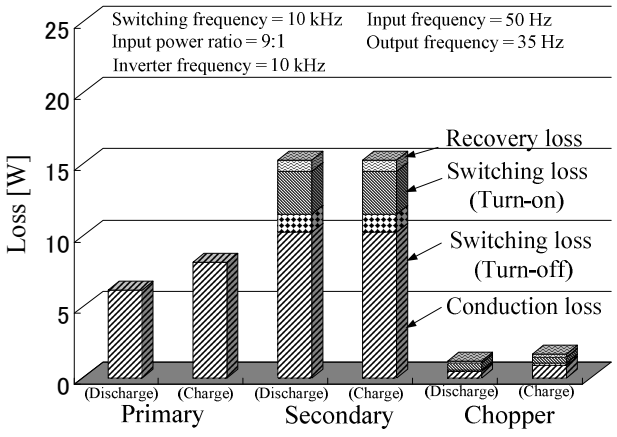

Fig. 14. Loss analysis – Switching device losses (Asymmetric method).

REFERENCES

[1] Anders Carlsson (1997), "The Back-to-back Converter - Design and Control", TEIE-1017, Industrial Electrical Engineering and Automation, Licentiate Theses 1998

[2] Gi-Taek Kim and Lipo T.A, "VSI-PWM Rectifier/Inverter System with a Reduced Switch Count", in *IEEE Industry Applications Conference*, Vol 3, pp 8-12, Oct 1995

[3] Imori. K, Shinohara. K, Muroya. M and Matsushita.Y, "Zero Switching Loss PWM rectifier of converter without DC link Components for Induction motor drive", in *Power Conversion Conference*, Japan, Vol 2, pp. 409-414, 2002

[4] Ogasawara. S, and Akagi. H, "Suppression of Common-mode Voltage in a PWM Rectifier/Inverter system", in *IEEE Industry Applications Conference,* Chicago, USA, Vol 3, pp. 2015-2021, Sept 2001

[5] Hyunjae Yoo, Kim J.H and Seung-Ki Sul, "Sensorless Operation of a PWM Rectifier for a Distributed Generation", *IEEE Trans. Power Electronics*, Vol 22, pp. 1014-1018, May 2007

[6] Yao Chen and XiMin Jin, "Modeling and Control of Three-phase Voltage Source PWM Rectifier", in *Power Electronics and Motion Control Conference*, Shanghai, Vol 3, pp.1-4, Aug 2006

[7] Hiquichi. Y, Yamamura. N, Ishida. M and Hori. T, "An Improvement of Performance for Small-Scaled Wind Power Generating System with Permanent Magnet Type Synchronous Generator", in *Industrial Electronic Society*, Japan, Vol 2, pp. 1037-1043, Oct 2000

[8] Z. Chen and E. Spooner, "Grid Power Quality with Variable Speed Wind Turbine", *IEEE Trans. on Energy Conversion*, Vol 16, No 2, June 2001

[9] Hao. S, Hunter.G, Ramsden. V and Patterson. D, "Control System Design for a 20kw Wind Turbine Generator with a Boost Converter and Battery Bank Load", in *Power Electronics Specialists Conference,* Canada, Vol 4, pp. 2203-2206, June 2001

[10] Wei. L, and Lipo. T.A, "A Novel Matrix Converter Topology with Simple Commutation", in *Industrial Electronic Society*, USA, Vol 3, pp. 1749-1754, Oct 2001.

[11] Jussila. M, Salo. M, Tuusa. H, "Realization of a Three-Phase Indirect Matrix Converter with an Indirect Vector Modulation Method", in *Power Electronics Specialist Conference*, Vol 2, pp. 689-694, June 2003

[12] Friedli. T, Heldwein. M.L, Giezendanner. F, and Kolar. J.W, "A High Efficiency Indirect Matrix Converter Utilizing RB-IGBTs", in *Power Electronics Specialist Conference*, pp. 1-7, June 2006

[13] Kolar. J.W, Schafmeister. F, Round. S.D, and Ertl. H, "Novel Three-Phase AC-AC Sparse Matrix Converters", *IEEE Trans. Power Electronics*, Vol 22, pp. 1649-1661, Sept. 2007

[14] Jun-ichi Itoh, and Fujita. K, "Novel Unity Power Factor Circuits Using Zero-Vector Control for Single-Phase Input Systems", *IEEE Trans. Power Electronics*, Vol 15, No. 1, January 2000

[15] Jun-ichi Itoh, Sato. I, Odaka. A, Ohguchi. H, Kodachi. H, and Eguchi. N, "A Novel Approach to Practical Matrix Converter Motor Drive System with Reverse Blocking IGBT", *IEEE Trans. Power Electronics*, Vol 20, pp. 1356-1363, Nov. 2005

[16] Jun-ichi Itoh, Ikuya. S, Hideki. O, Kazuhisa. S, Akihiro. O, and Naoya. E, "A Control Method for The Matrix Converter based on virtual AC/DC/AC Conversion Using Carrier Comparison Method", *IEE Trans. in Japan*, Vol 152, pp. 65-73, Jun 2005

[17] Jun-ichi Itoh, and Kato. K, "Control Method for A Three-port Interface Converter Using an Indirect Matrix Converter with an Active Snubber Circuit", in *Power Electronics and Motion Control Conf. 2008*, pp. 581-588, Sept 2008.

[18] Jun-ichi Itoh, Iida. T, and Odaka. A, "Realization of High Effieiency AC Link Converter System Based on AC/AC Direct Conversion Techniques with RB-IGBT", in *IEEE Industrial Electronics Conf.*, Paris, pp. 1703-1708, Nov. 2006

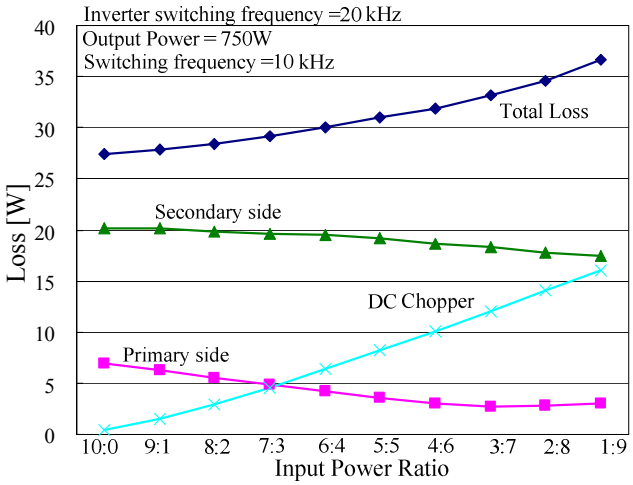

Fig. 15. Loss analysis – Changes in input ratio (Symmetric method).

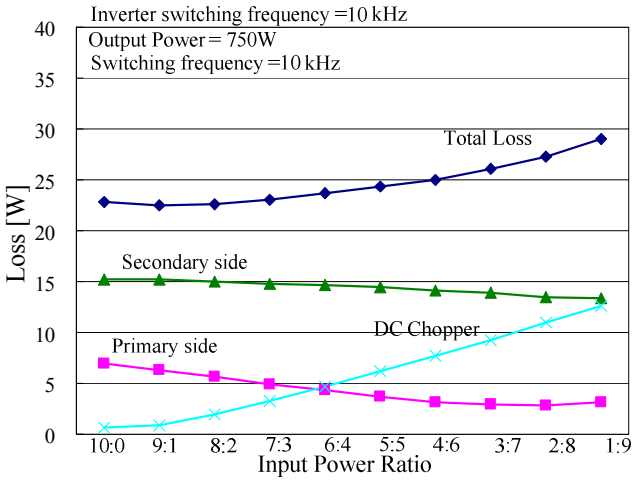

Fig. 16. Loss analysis – Changes in input power ratio (Asymmetric method).